JOURNAL OF SOLID STATE CHEMISTRY **123,** 255–266 (1996)
ARTICLE NO. 0176

Chemical and Magnetic Characterization of Spinel Materials in the $LiMn_2O_4$–$Li_2Mn_4O_9$–$Li_4Mn_5O_{12}$ System

Christian Masquelier,*,[1] Mitsuharu Tabuchi,† Kazuaki Ado,† Ryoji Kanno,‡ Yo Kobayashi,§ Yuzuru Maki,‖ Osamu Nakamura,† and John B. Goodenough*

*Center for Materials Science and Engineering, University of Texas at Austin, ETC 9.126, Austin, Texas 78712-1063; †Osaka National Research Institute, 1-8-31 Midorigaoka, Ikeda, Osaka 563, Japan; ‡Kobe University, Rokkoudai-cho, Nada, Kobe, Hyogo 657, Japan; §Central Research Institute of Electric Power Industry, 2-11-1 Iwado Kita, Komae, Tokyo, Japan; and ‖Rigaku Corporation, 14-8 Akaoji-cho, Takatsuki, Osaka 569, Japan

Received December 29, 1995; in revised form February 8, 1996; accepted February 14, 1996

Lithium manganospinels belonging to the $LiMn_2O_4$–$Li_2Mn_4O_9$–$Li_4Mn_5O_{12}$ system were prepared by solid-state reaction of various lithium salts and manganese sources at temperatures ranging from 400 to 900°C. Their exact stoichiometry, which is highly dependent on the preparation temperature, was determined by X-ray diffraction, atomic absorption spectroscopy, and redox titration. Nearly stoichiometric $LiMn_2O_4$ shows a reversible phase transition at 30°C upon heating and at 10°C upon cooling, which is associated with a tetragonal-cubic transformation. An increase in the average oxidation state of manganese from 3.5+ to 4+ in the two systems $Li_{1-\delta}Mn_{2-2\delta}$ ($0 \leq \delta \leq 0.11$) and $Li_{1+\delta}Mn_{2-\delta}O_4$ ($0 \leq \delta \leq 0.33$) results in (i) the suppression of the Jahn–Teller distortion observed around room temperature for stoichiometric $LiMn_2O_4$ and (ii) a progressive passage from antiferromagnetic ($LiMn_2O_4$, $\theta = -266$ K, $n_{Mn}+ = 3.5$) to ferromagnetic behavior ($Li_4Mn_5O_{12}$, $\theta = +40$ K, $n_{Mn}+ = 4.0$), where the lattice parameter is not too small.

INTRODUCTION

Over the past 15 years, increasing efforts to identify electrode materials for light and compact rechargeable battery systems have led to the widespread use of oxides of transition-metal elements (Co, Ni, Mn, V, Fe) as hosts for the deintercalation/intercalation of lithium from/into cathodes of secondary batteries. First proposed in 1980 (1), $LiCoO_2$ was successfully developed by SONY Energytec as the cathode material of the first rechargeable ''Rocking-Chair'' battery system commercialized in 1991 (2). $LiCoO_2$ (as well as $LiMO_2$, M = Ni, V, Cr), adopts a layered rock-salt structure that provides a 2-D array of edge-sharing LiO_6 octahedra, favorable for a reversible extraction/insertion of lithium. The concept of using anion (oxygen) close-packed structures was further extended by Goodenough's group to 3-D materials with the spinel structure (3). It was shown that lithium could be intercalated into the spinels $Fe^{3+}[Fe^{2+}Fe^{3+}]O_4$ (inverse) (4) and $Mn^{2+}[Mn^{3+}Mn^{3+}]O_4$ (normal) (5), and either inserted or extracted into/from the normal spinel $Li[Mn_2]O_4$ (5, 6). Due to their lower cost and toxicity, as compared to those of cobalt, nickel, or vanadium, the oxides of lithium and manganese, $LiMn_2O_4$ (7–11), $Li_4Mn_5O_{12}$ (12, 13), $Li_2Mn_4O_9$ (14–16), and $LiMnO_2$ (17–21), remain among the most promising materials as 3–4 V vs Li/Li^+ cathodes for rechargeable lithium batteries.

Among these options, the spinel $LiMn_2O_4$ ($Li_{(8a)}[Mn_2]_{(16d)}O_4$) has been the most extensively studied: electrochemical extraction of one lithium ion from the tetrahedral (8*a*) sites occurs in two steps at approximately 4 V vs Li/Li^+ ($LiMn_2O_4 \rightarrow Mn_2O_4$ (λ-MnO_2)) whereas the insertion of one lithium ion into the octahedral (16*c*) site occurs at approximately 3 V vs Li/Li^+ ($LiMn_2O_4 \rightarrow Li_2Mn_2O_4$ ($LiMnO_2$)). The insertion of lithium into $LiMn_2O_4$, toward $Li_2Mn_2O_4$, is naturally accompanied by a reduction of the average oxidation state of manganese from 3.5 to 3: the presence of more than 50% of Jahn–Teller ions (Mn^{3+}) in the host structure introduces a cubic to tetragonal distortion (from $c/a = 1$ to $c/a = 1.16$, $\Delta V/V = 6\%$, (5)), which, upon repeated cycles, is believed to deteriorate the electrical contact between the surfaces of the insertion-material particles and hence to decrease the capacity of the cathode (13).

The ''defect'' spinel $Li_2Mn_4O_9$ (more correctly described as $Li_{0.89}\square_{0.11}[Mn_{1.78}\square_{0.22}]O_4$) and the ''stoichiometric'' spinel $Li_4Mn_5O_{12}$ show much better electrochemical cyclability at 3 V than $LiMn_2O_4$ (12, 15). A significant insight into the electrochemical behavior of lithium manganospinels was recently provided by Gummow *et al.* (13), who considered the $LiMnO_2$–Li_2MnO_3–MnO_2 phase diagram slightly adapted here in Fig. 1. Both $Li_2Mn_4O_9$ and $Li_4Mn_5O_{12}$ are

[1] To whom correspondence should be addressed.

0022-4596/96 $18.00

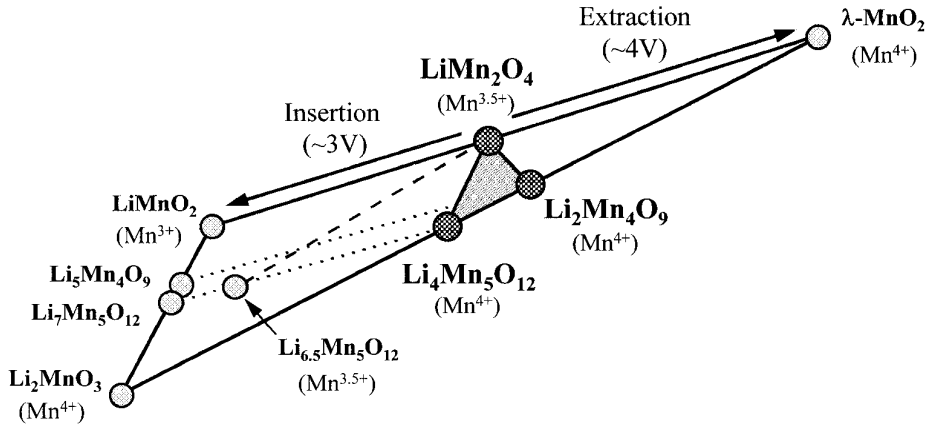

FIG. 1. Part of the Li–Mn–O system. Reprinted from *Solid State Ionics* **69,** R. J. Gummow, A. DeKock, and M. M. Thackeray, pages 59–67 (1994) with kind permission of Elsevier Science.

characterized by an oxidation state of manganese equal to 4+ and, accordingly, possess no theoretical capacity on charge at 4 V against Li/Li^+. On the other hand, the high oxidation state of manganese allows for the insertion of significant quantities of lithium into the spinel structure (toward $Li_5Mn_4O_9$ and $Li_7Mn_5O_{12}$, respectively), before the onset of the Jahn–Teller effect, represented in Fig. 1 by the dashed line joining the $LiMn_2O_4$ and $Li_{6.5}Mn_5O_{12}$ compositions. Of particular interest is the shaded region $LiMn_2O_4$–$Li_2Mn_4O_9$–$Li_4Mn_5O_{12}$, from which two joins can be described:

(i) The defect spinels $Li_{1-\delta}Mn_{2-2\delta}O_4$ ($0 \leq \delta \leq 0.11$) of the join $LiMn_2O_4$–$Li_2Mn_4O_9$ contain vacancies on both the (8*a*) lithium sites and the (16*d*) manganese sites. Such compositions are characterized by a constant ratio Li/Mn $= \frac{1}{2}$. Their stoichiometry, i.e., the manganese average oxidation state, depends essentially on the temperature at which the solid-state reaction is carried out: an increase in the firing temperature progressively reduces the manganese from Mn^{4+} ($Li_2Mn_4O_9$, prepared at 400°C) to an average value of $Mn^{3.5+}$ ($LiMn_2O_4$, prepared at $T = 850$°C). It is important to realize that lithium manganospinels, which are improperly referred to as ''low-temperature $LiMn_2O_4$,'' show good electrochemical properties that are more likely to be related to intrinsic parameters such as the oxidation state of manganese, the value of the lattice parameter *a*, and the distribution of lithium and manganese cations on the tetrahedral and octahedral sites, rather than to extrinsic parameters such as the size of the spinel particles. The higher δ, the lower the capacity at 4 V, the smaller *a*, and the better the cyclability at 3 V vs Li/Li+ (16).

(ii) In the stoichiometric spinels $Li_{1+\delta}Mn_{2-\delta}O_4$ ($0 \leq \delta \leq 0.33$) of the join $LiMn_2O_4$–$Li_4Mn_5O_{12}$, lithium partly substitutes for manganese on the octahedral (16*d*) sites. ''Stoichiometric'' is used here to signify that the spinel cation/anion ratio is still kept constant to 3/4. The cubic lattice parameter *a* was reported to decrease as a function of δ, from $a = 8.232$ Å ($\delta = 0$) to $a = 8.137$ Å ($\delta = 0.33$), as the result of a combined effect of the increase in the average oxidation state of manganese (from 3.5+ to 4+) and of the substitution of manganese by lithium on the octahedral sites (13). Despite their lower capacities at 4 V when compared with stoichiometric $LiMn_2O_4$, slightly lithium-rich $Li_{1+\delta}Mn_{2-\delta}O_4$ compositions (for example, $\delta = 0.05$) show better capacity retention during cycling. This was reported by Gummow *et al*. to be caused by a smaller volume change between charged and discharged compositions and by the absence of any possibility of Jahn–Teller deformation at the end of discharge (13). An alternative explanation was recently proposed by Xia *et al.* (22). Despite some uncertainties concerning the real composition of their material, i.e., $Li_{1.04}Mn_2O_{4.14}$ should not be written as $Li_{1+x}Mn_2O_4$, these authors suggest that the capacity fading on cycling stoichiometric $LiMn_2O_4$ toward $Li_{1-x}Mn_2O_4$ is mainly due to the existence of a two-phase region at the end of the charge ($0.7 \leq x \leq 0.9$), whereas a single-phase process with high reversibility is observed for $Li_{1.04}Mn_2O_{4.14}$.

It is crucial to realize that the preparation of such materials in a reproducible manner with close control of their stoichiometry is far from trivial due, in particular, to the similar stability in air of manganese as either Mn^{3+} or Mn^{4+} in an octahedral environment. In fact, depending on the temperature at which the spinel phases are prepared, as well as on the exact starting Li/Mn ratio of the samples, impurities such as Li_2MnO_3 may be obtained in addition to compositions lying in the $LiMn_2O_4$–$Li_2Mn_4O_9$–$Li_4Mn_5O_{12}$ phase field. Their identification is made difficult by the extreme similarity of their X-ray diffraction patterns. Several complementary chemical and physical characterizations of the lithium manganospinel materials are therefore needed (Li/Mn ratio, Mn oxidation state, and cubic lattice parameter) prior to discussion of their performances as

cathode materials for rechargeable lithium batteries. The objective of this work was to provide a systematic characterization of the formation of spinel materials with compositions belonging to the $LiMn_2O_4$–$Li_2Mn_4O_9$–$Li_4Mn_5O_{12}$ system. Toward this end, we carried out solid-state reactions between different lithium salts ($LiOH \cdot H_2O$, Li_2CO_3) and manganese sources ($MnCO_3$, MnOOH, MnO_2) at temperatures ranging from 400 to 900°C. Particular attention was paid to control systematically the lattice parameters and the average oxidation state of manganese in different spinel compositions. The effect of small stoichiometry changes on the existence of the Jahn–Teller cubic–tetragonal distortion and on the magnetic properties of lithium manganospinels is discussed.

EXPERIMENTAL

Synthesis. All the samples were prepared by reacting thoroughly mixed lithium salts ($LiOH \cdot H_2O$, Li_2CO_3, or $LiNO_3$) and manganese sources ($MnCO_3$, MnOOH, or MnO_2—E.M.D.) in air for 48 h at temperatures ranging from 400 to 900°C. The samples were ground twice between firings and finally cooled (5°C/min) down to room temperature. The "A" and "B" series of materials that we describe in this paper represent attempts to prepare compositions on the joins $LiMn_2O_4$–$Li_2Mn_4O_9$, and $LiMn_2O_4$–$Li_4Mn_5O_{12}$, respectively. The A samples were obtained by reacting stoichiometric mixtures with the Li/Mn ratio = $\frac{1}{2}$, at temperatures ranging from 400 to 900°C; the B samples were obtained by reacting stoichiometric mixtures of $LiOH \cdot H_2O$ and MnOOH with the Li/Mn ratio varying from $\frac{1}{2}$ to 4/5, at 400, 450, and 650°C.

X-ray diffraction. The X-ray diffraction patterns were recorded at 103, 298, and 323 K on a Rigaku Rotaflex/RINT Rotating Anode diffractometer with the Cu$K\alpha$ radiation. The spinel compositions were indexed in the cubic space group $Fd3m$. The unit-cell parameter a was calculated from eight d_{hkl} values previously corrected for systematic deviation by using Si as an internal standard.

Thermal analysis. Thermogravimetric experiments (TG) were performed on the starting materials $MnCO_3$, MnOOH, and MnO_2 (E.M.D.), with a Rigaku-TG8101D thermal analyzer. Samples of approximately 40 mg were placed in Pt crucibles, heated in air up to 800°C and cooled down to room temperature at a rate of approximately 10°C/min. Differential scanning calorimetry experiments were performed in air between 233 and 393 K with a Rigaku TAS-200 thermal analyzer.

Chemical analysis. The lithium/manganese content in the product spinels was determined with atomic absorption spectroscopy. The average oxidation state of manganese was determined with a procedure previously described by Wickham (23). To this end, a standard aqueous solution S_1 of $VOSO_4 \cdot 3H_2O$, 7.5×10^{-2} N, in 1.8 N H_2SO_4 was prepared. The $Li_xMn_y^{n+}O_{(x+ny)/2}$ samples (~50 mg) were dissolved into an excess of S_1 (25 ml): At this stage, Mn^{n+} was reduced to Mn^{2+}, and part of V^{4+} was oxidized to V^{5+}. After addition of ~5 ml of concentrated H_3PO_4, the excess of V^{4+} in the solution was determined by potentiometric titration with a standard solution S_2 of $KMnO_4$, 5×10^{-2} N.

Magnetic measurements. The magnetic susceptibility measurements were performed in He atmosphere between 83 and 300 K with a MB-3 Shimazu Faraday balance under a maximum magnetic field at 12.5 kOe. Mn Tutton's salt ($(NH_4)_2Mn(SO_4)_2 \cdot 6H_2O$, reagent grade) was used as the standard substance for the calibration of the magnetic susceptibility determinations. The temperature and magnetic field dependence of the magnetization were measured between 5 and 300 K with a SQUID magnetometer (MPMS2, Quantum Design).

RESULTS AND DISCUSSION

(*a*) *Preparation and Chemical Characterization of Defect Spinels* $Li_{1-\delta}Mn_{2-2\delta}O_4$

The A samples of the $LiMn_2O_4$–$Li_2Mn_4O_9$ join have lithium and manganese vacancies on the (8*a*) tetrahedral and (16*d*) octahedral sites, respectively, and are characterized by a constant Li/Mn ratio Li/Mn = $\frac{1}{2}$. Figure 2 shows the variation of the manganospinel cubic lattice parameter a versus the firing temperature for three series of A samples (Li/Mn = $\frac{1}{2}$) obtained by solid-state reaction of stoichiometric mixtures of $LiOH \cdot H_2O$ and as received $MnCO_3$, MnOOH (Manganite, TOSOH Corp.), or MnO_2 (E.M.D.). The vertical dotted line delineates the low-temperature region ($T < \sim 620$°C) where the lithium manganospinel is systematically accompanied by impurities such as β-MnO_2, Li_2MnO_3, or Mn_2O_3, as clearly seen in Fig. 3.

The formation of $Li_{1-\delta}Mn_{2-2\delta}O_4$ materials (Li/Mn = $\frac{1}{2}$) via $LiOH \cdot H_2O$ and MnOOH at temperatures ranging from 400 to 900°C takes place as follows: At 400°C, samples consisting of pure lithium manganospinels could not be obtained. Together with a spinel phase of unknown composition, impurities such as β-MnO_2 (JCPDS 24-735), Ramsdellite R-MnO_2 (JCPDS 39-0375), and Li_2CO_3 are clearly identified. This confirms earlier observations of de Kock *et al.* (14) and Thackeray *et al.* (16) according to which the preparation of the fully oxidized $Li_2Mn_4O_9$ ($y = 4$ in the Li_2O–y MnO_2 system) may strongly depend on the starting materials, the reaction time, and the oxygen partial pressure surrounding the reaction. The presence of β-MnO_2, which results from the decomposition of MnOOH according to

$$MnOOH \rightarrow MnO_2 + 1/2\ H_2\uparrow \qquad [1]$$

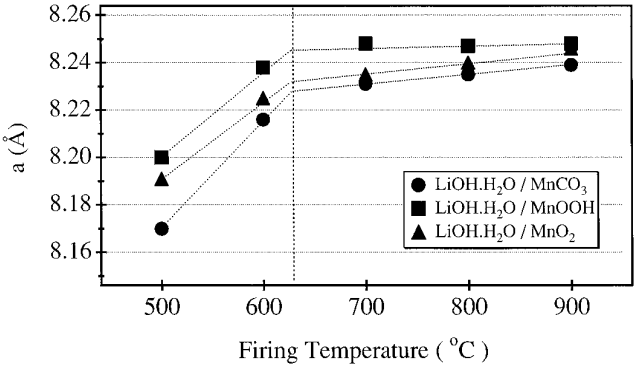

FIG. 2. Spinel cubic lattice parameter *a* versus preparation temperature for A samples (Li/Mn ~ 1/2).

is even more obvious at 450°C, where a spinel phase of poor crystallinity and small lattice parameter ($a < 8.20$ Å) is also formed. At these low temperatures, manganese is stable preferentially as Mn^{4+}, and there is competition between the formation of a defect-spinel $Li_{1-\delta}Mn_{2-2\delta}O_4$ (δ close to 0.11) and Li_2MnO_3 according to

$$4\,MnO_2 + Li_2O \rightarrow Li_2Mn_4O_9 \qquad [2]$$

$$MnO_2 + Li_2O \rightarrow Li_2MnO_3. \qquad [3]$$

A further increase of the reaction temperature, i.e., 500°C, induces a progressive reduction of Mn^{4+} to Mn^{3+}; two main reactions may be considered:

$$Li_2Mn_4O_9 \rightarrow 2\,LiMn_2O_4 + 1/2\,O_2\uparrow \qquad [4]$$

$$2\,MnO_2 \rightarrow Mn_2O_3 + 1/2\,O_2\uparrow. \qquad [5]$$

Indeed, we do observe Mn_2O_3 (bixbyite) and an increase in the *a* lattice parameter of the spinel phase. This corroborates earlier observations of Macklin *et al.* (15) who reported the presence of Mn_2O_3 impurities up to $T = 600$°C together with an increase of the spinel *a* parameter from 8.190 (450) to 8.231 Å (600°C). Although hardly detectable on the XRD patterns, small quantities of orange-colored Li_2MnO_3 particles were still observed in the 500 and 600°C

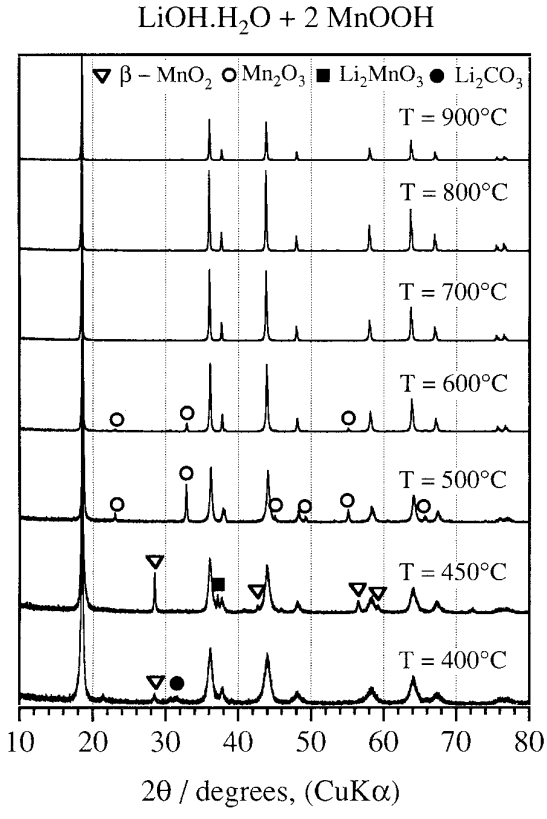

FIG. 3. Powder X-ray diffraction patterns of A samples obtained by reaction of $LiOH \cdot H_2O$ + 2 MnOOH.

TABLE 1
Characterization of Lithium Manganospinels in the $LiMn_2O_4$–$Li_2Mn_4O_9$ System

Sample	Starting materials	Firing temperature (°C)	Li/Mn	*a* (Å)	*x* in $Li_2Mn_4O_{8+x}$	δ in $Li_{1-\delta}Mn_{2-2\delta}O_4$	Mn oxidation state
A1	$MnOOH/LiOH \cdot H_2O$	700	1/2	8.248(2)	0.05	0.006	3.53
A2	$MnOOH/LiOH \cdot H_2O$	800	1/2	8.247(1)	0.06	0.007	3.53
A3	$MnOOH/LiOH \cdot H_2O$	900	1/2	8.248(1)	0.01	0.001	3.51
A4	$MnOOH/Li_2CO_3$	400	1/2	8.204(3)	0.39	0.047	3.69
Sample	Starting materials	Firing temperature	Li/Mn	*a* (Å)	*x* in $Li_{2.04}Mn_{3.96}O_{8+x}$	δ in $Li_{1.04(1-\delta)}Mn_{2(1-\delta)}O_4$	Mn oxidation state
A5	$MnCO_3/LiOH \cdot H_2O$	700	1.04/2	8.231(2)	0.17	0.031	3.61
A6	$MnCO_3/LiOH \cdot H_2O$	800	1.04/2	8.235(1)	0.05	0.017	3.55
A7	$MnCO_3/LiOH \cdot H_2O$	900	1.04/2	8.239(1)	0.07	0.020	3.56

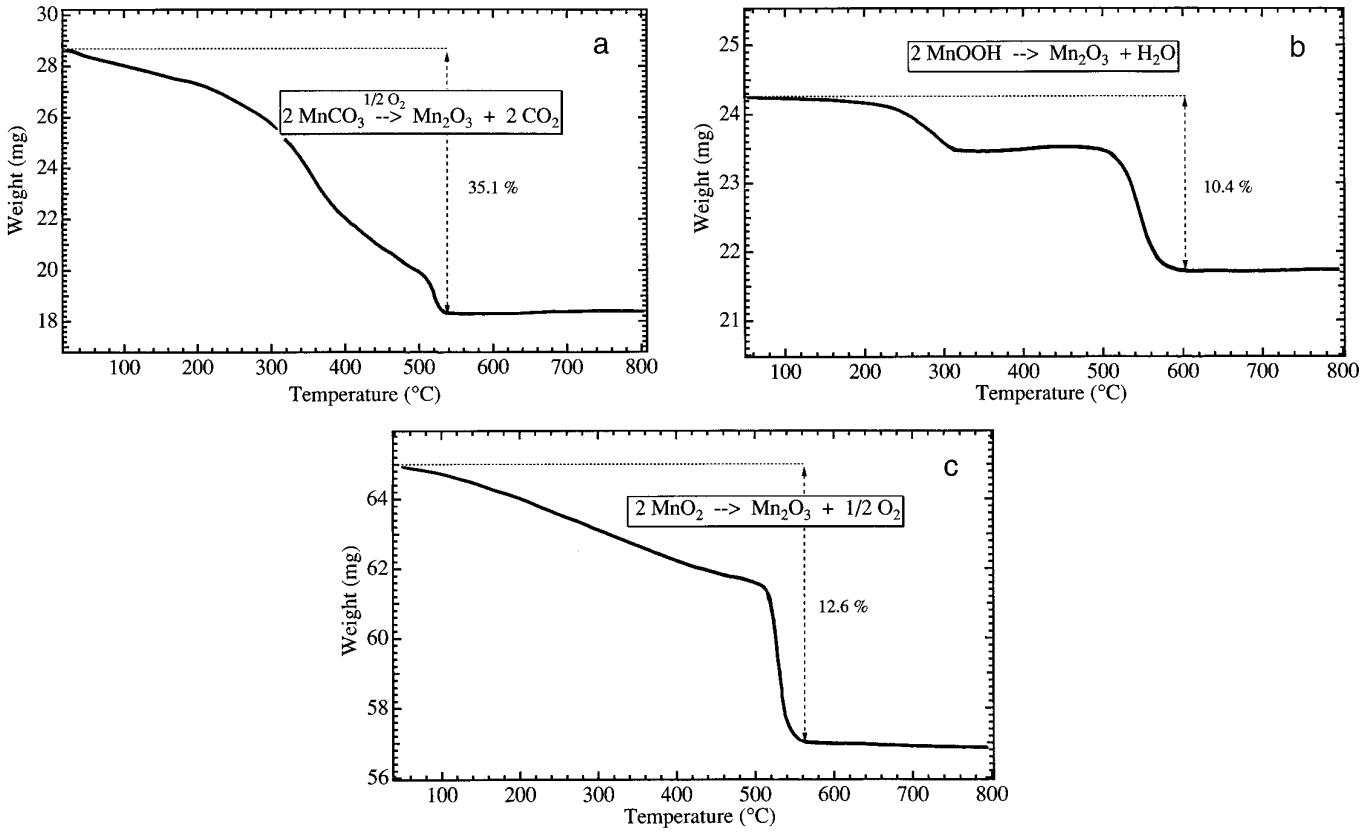

FIG. 4. Thermogravimetric curves of the decomposition in air of (a) $MnCO_3$, (b) MnOOH, and (c) MnO_2. The observed weight losses which lead in every case to Mn_2O_3 are indicated in %.

samples. The materials obtained after firing at $T = 700$, 800, and 900°C (A1, A2, and A3) are pure lithium manganospinels of composition $Li_{1-\delta}Mn_{2-2\delta}O_4(\delta \leq 0.007)$, as determined by atomic absorption spectroscopy and manganese-oxidation-state titration (Table 1). They have, within experimental uncertainty, very similar lattice parameters and manganese oxidation state. Unequivocally, this shows that stoichiometric $LiMn_2O_4$ can be prepared at 700°C from MnOOH and $LiOH \cdot H_2O$ as starting materials. The consistency between the chemical analysis results and the measured cubic lattice parameters demonstrates also the accuracy of the titration method proposed by Wickham and Whipple and its usefulness in precisely determining the real stoichiometry of lithium manganospinels. Additionally, these results tend to demonstrate and to definitely establish that spinel materials with $a < 8.245$ Å should not be considered as having the $LiMn_2O_4$ stoichiometry but instead as having a stoichiometry which lies either on the join $LiMn_2O_4$–$Li_{0.89}\square_{0.11}[Mn_{1.78}\square_{0.22}]O_4$ ($Mn^{3.5+}$ to Mn^{4+}) if the Li/Mn ratio is $\frac{1}{2}$, or within the shaded region of Fig. 1 ($LiMn_2O_4$–$Li_2Mn_4O_9$–$Li_4Mn_5O_{12}$) for a Li/Mn ratio $> \frac{1}{2}$.

Figure 2 also shows that the two series of A spinel materials obtained via $MnCO_3$ or MnO_2 (E.M.D.) present, at a given temperature, a lower a lattice parameter, and hence a higher manganese oxidation state, than A spinels prepared under the same conditions via MnOOH. At low temperature, where the nature and the morphology of the starting materials play an important role, these differences may be explained by the differences in oxidation state of Mn and in the reactivities of Li_2O toward manganese sources of various particle sizes and shapes. It appeared, however, in the course of our study that both starting materials $MnCO_3$ and MnO_2 were not of exact stoichiometry, as demonstrated in Fig. 4 by their thermogravimetric (TG) decomposition curves recorded between room temperature and 800°C in air. The three decompositions

$$2\,MnCO_3 \xrightarrow{1/2\,O_2} Mn_2O_3 + 2\,CO_2\uparrow, \quad [6]$$

$$2\,MnOOH \rightarrow Mn_2O_3 + H_2O\uparrow, \quad [7]$$

and

$$2\,MnO_2 \rightarrow Mn_2O_3 + \tfrac{1}{2}\,O_2\uparrow \quad [8]$$

correspond to theoretical weight losses of 31.3, 10.2, and 9.2%, respectively. Our experimental values of 35.1, 10.4, and 12.6% indicate that both the $MnCO_3$ and MnO_2 start-

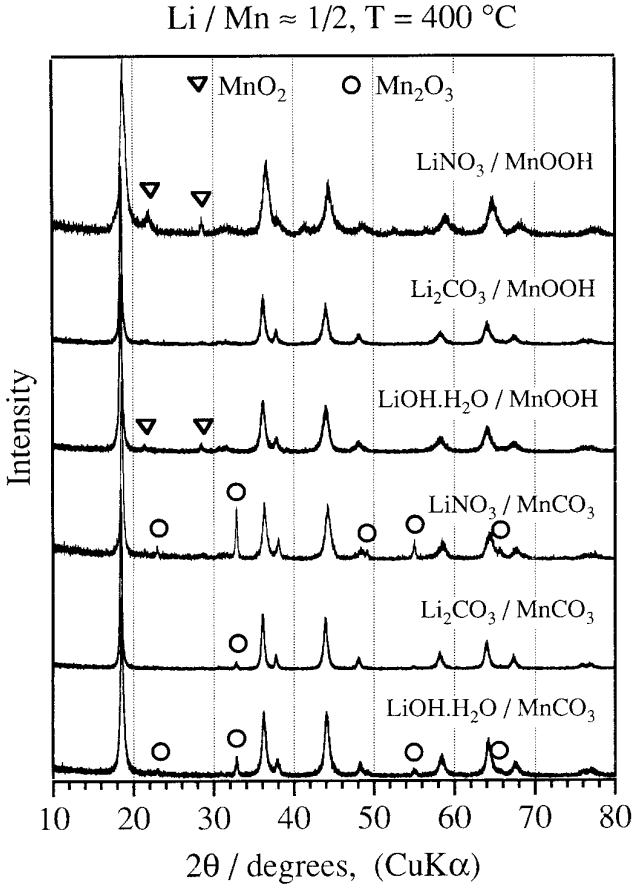

FIG. 5. Powder X-ray diffraction patterns of A samples obtained by reaction of various lithium salts and manganese sources in air at 400°C.

ing materials that we used were not purely stoichiometric and probably contained surface and/or constitutional water. This resulted in preparing spinel compositions slightly richer in lithium than originally intended, with a Li/Mn ratio equal to 1.04/2 instead of 1/2. The values of the average manganese oxidation state (3.56+) and lattice parameter a = 8.239(1) Å for the A7 sample obtained by reacting $MnCO_3$ and LiOH · H_2O at 900°C can be fully understood on the basis of such initial Li/Mn nonstoichiometric ratio.

To provide further evidence of the importance of the choice of the starting materials for obtaining pure highly oxidized lithium manganospinels at low temperature, we regroup in Fig. 5 the X-ray diffraction patterns of the reaction products of three different lithium salts ($LiNO_3$, LiOH · H_2O, and Li_2CO_3) reacted at 400°C with either $MnCO_3$ or MnOOH, with initial stoichiometry Li/Mn = 1/2. The three spinel phases obtained from $MnCO_3$ as the manganese source are accompanied by Mn_2O_3 as the major impurity, particularly if $LiNO_3$ is used as the starting lithium salt. The sample obtained via $MnCO_3$ and Li_2CO_3 shows only a little of impurity phases and, as suggested by Thackeray *et al.* (16), longer reaction times (~96 h) are necessary to obtain a pure lithium manganospinel with high manganese oxidation state. The samples obtained from MnOOH instead of $MnCO_3$ do not contain any Mn_2O_3 impurity, but rather MnO_2 (for two of them), as a result of the oxidation of MnOOH. The sample labeled A4 in Table 1, obtained from Li_2CO_3 and MnOOH, corresponds to our only successful attempt so far to obtain by solid-state reaction at 400°C a pure lithium manganospinel material $Li_{1-\delta}Mn_{2-2\delta}O_4$ of composition close to $Li_2Mn_4O_9$ ($\delta = 0.11$). The lattice parameter a = 8.204 (3) Å is consistent with the chemical formula $Li_{1-\delta}Mn_{2-2\delta}O_4$ ($\delta = 0.047$) determined by chemical analysis, which corresponds to an average oxidation state of manganese $n^+_{Mn} = 3.69$ in the spinel material. These values are intermediate between those reported for $LiMn_2O_4$ ($\delta = 0$, a = 8.248 Å, $n^+_{Mn} = 3.50$) (24) and $Li_2Mn_4O_9$ ($\delta = 0.11$, a = 8.162 Å, $n^+_{Mn} = 4.00$) (16). These results confirm that the defect spinels $Li_{1-\delta}Mn_{2-2\delta}O_4$ are difficult to prepare with a precise, predetermined composition, but additionally show that simple X-ray diffraction or oxido-reduction titration can, in fact, provide reliable direct characterization of their exact stoichiometry.

(*b*) *Preparation and Characterization of Stoichiometric Spinels* $Li_{1+\delta}Mn_{2-\delta}O_4$

The B samples of the $LiMn_2O_4$–$Li_4Mn_5O_{12}$ ($\delta = 0.33$) join are characterized by a progressive substitution of Mn by Li on the (16*d*) octahedral sites; accordingly, the average oxidation state of manganese is increased from 3.5+ to 4+. Figure 6 shows the variation of the manganospinel cubic lattice parameter a with the nominal compositions δ in stoichiometric spinel materials $Li_{1+\delta}Mn_{2-\delta}O_4$ for three series of B samples prepared by the solid-state reaction of $(2 - \delta)$ MnOOH and$(1 + \delta)$ LiOH · H_2O at 400, 450, and

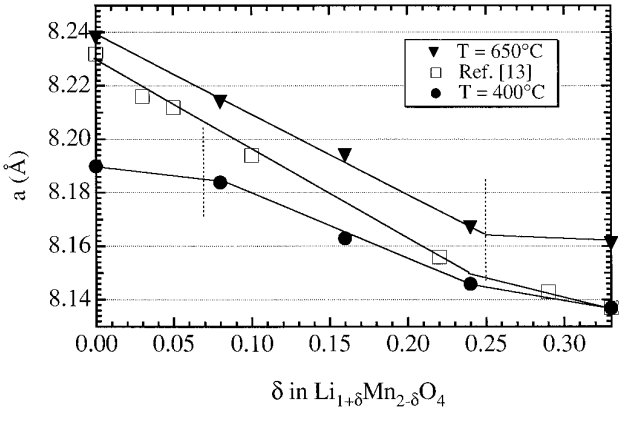

FIG. 6. Spinel lattice parameter a versus nominal composition δ in $Li_{1+\delta}Mn_{2-\delta}O_4$ samples prepared at 400 (●) and 650°C (▼). Open symbols: corresponding data reported in Ref. (13).

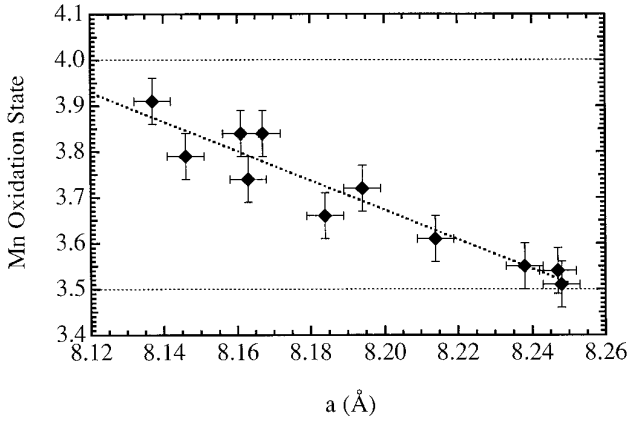

FIG. 7. Manganese oxidation state determined by redox titration versus lattice parameter for samples of nominal composition $Li_{1+\delta}Mn_{2-\delta}O_4$ ($0 \le \delta \le 0.33$), prepared by solid-state reaction of MnOOH and $LiOH \cdot H_2O$ between 400 and 650°C.

650°C. We included, for comparative purpose, the values reported by Gummow *et al.* (13) for samples of nominal compositions $Li_{1+\delta}Mn_{2-\delta}O_4$ reacted at 650°C for $\delta < 0.22$ and at $T = 450$°C for $\delta = 0.22$ and 0.29. It is readily apparent from Fig. 7 that the value of the average oxidation state in the spinel phase is closely related to the value of the cubic lattice parameter, which varies from $a = 8.248$ Å ($n^+_{Mn} = 3.5$) to $a = 8.137$ Å ($n^+_{Mn} = 3.91$). The spinel phase formation on the join $LiMn_2O_4$–$Li_4Mn_5O_{12}$ is also clearly temperature dependent, i.e., Mn^{4+}-rich compositions will form preferentially at low temperatures.

It is one of the objectives of this paper to particularly insist on the high sensitivity of lithium manganospinels toward oxidizing/reducing atmospheres as well as toward the temperature at which the samples are prepared. Very recent literature shows that efforts and attention need still to be made by the chemist, the physicist, and the electrochemist to establish unequivocally the chemical composition of these spinel materials before undertaking any serious discussion of their structural or electrochemical behavior. As a general trend, it is clear from Fig. 6 that a higher preparation temperature will result in a more reduced manganese cation, as we pointed out in the previous section. To illustrate this, it is important to realize that the sample labeled B5 in Table 2, although prepared from a stoichiometric ratio Li/Mn = 4/5, does not have the composition $Li_4Mn_5O_{12}$. In fact, the X-ray diffraction pattern of sample B5 clearly shows the appearance of extra diffraction peaks at $2\theta \simeq 37°$, 45°, and 65° due to the presence of Li_2MnO_3, detectable as well by the presence of characteristic orange-colored particles at the surface of the spinel material. The average oxidation state of manganese is $n^+_{Mn} = 3.84$ instead of $n^+_{Mn} = 4$. This accounts for the abnormally high value of the lattice parameter $a = 8.161$ Å, as identified by the break in the continuous decrease of a with δ in Fig. 6. At 400°C, for the same stoichiometric starting mixture with Li/Mn = 4/5, a slightly more oxidized, pure spinel material B10 was obtained with $n^+_{Mn} = 3.91$ and $a = 8.137$ Å, very close to the values reported by Gummow *et al.* (13) and Richard *et al.* (10) for $Li_4Mn_5O_{12}$. This also supports de Kock *et al.*'s observation (14) that the stability of Mn^{4+} spinel phases in the system Li_2O–y MnO_2 increases from $y = 2.5$ ($Li_4Mn_5O_{12}$) to $y = 4$ ($Li_2Mn_4O_9$) as the concentration of the MnO_2 component decreases. Intuitively, it may be easily understood that, at the relatively low temperatures required ($T \simeq 400$°C) to keep a high oxidation state for manganese, the formation of a defect spinel $Li_{0.89}\square_{0.11}[Mn_{1.78}\square_{0.22}]O_4$ with a high concentration of vacancies on both tetrahedral and octahedral sites will be much more difficult than the formation of a stoichiometric spinel $Li_{1.00}[Mn_{1.67}Li_{0.33}]O_4$ where lithium has no difficulty to substitute for manganese on the (16*d*) octahedral site (26). The left part of Fig. 6 is related to compositions with the Li/Mn ratio close to 1/2, hence close to $LiMn_2O_4$. As discussed in detail in the previous section, we could not obtain a pure spinel sample by solid-state reaction of 2 MnOOH + $LiOH \cdot H_2O$ at 400°C. Sample B6 is a mixture of MnO_2 impurities and a defect spinel of composition $Li_{1-\delta}Mn_{2-2\delta}O_4$ with a small lattice parameter ($a = 8.190$ Å), due to a relatively large oxidation state of manganese.

(*c*) *Jahn–Teller Deformation in $LiMn_2O_4$ around Room Temperature*

The existence of a lattice distortion from cubic to tetragonal symmetry in manganese oxide spinels was characterized in the past (27). It occurs due to the presence in the oxide of a critical concentration of Jahn–Teller ions Mn^{3+} ($d^4 : t_2^3 e^1$) where an energetically favorable *e* orbital degen-

TABLE 2
Characterization of Lithium Manganospinels in the $LiMn_2O_4$–$Li_4Mn_5O_{12}$ System

Sample	Firing temperature	Nominal δ in $Li_{1+\delta}Mn_{2-\delta}O_4$	a (Å)	Mn oxidation state
B1	650	0	8.238(2)	3.53
B2	650	0.08	8.214(1)	3.61
B3	650	0.16	8.194(1)	3.72
B4	650	0.24	8.167(3)	3.84
B5	650	0.33	8.161(3)	3.84
B6	400	0	8.190(2)	#
B7	400	0.08	8.184(2)	3.66#
B8	400	0.16	8.163(2)	3.74
B9	400	0.24	8.146(2)	3.79
B10	400	0.33	8.137(3)	3.91

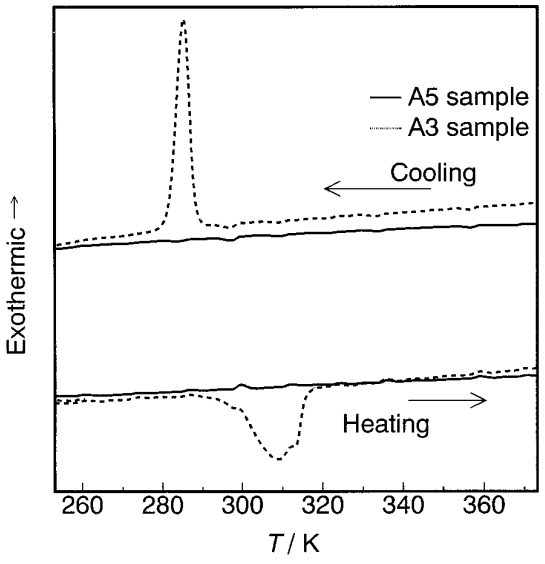

FIG. 8. Different scanning calorimetry curves of stoichiometric $LiMn_2O_4$ A3 (dashed lines) and $Li_{1.01}Mn_{1.94}O_4$ A5 (full lines), recorded after a preliminary heating up to 393 K.

eracy induces a cooperative distortion throughout the crystal. This phenomenon was clearly identified, for example, for the tetragonal spinel Mn_3O_4 ($Mn^{2+}[Mn^{3+}Mn^{3+}]O_4$, $c/a = 1.16$) (3, 5, 27). $LiMn_2O_4$, which contains a critical concentration of 50% Mn^{3+} ($n^+_{Mn} = 3.50$), is at the border of the cubic ↔ tetragonal transformation domain at room temperature. Consequently, after only small amounts of lithium are inserted into $LiMn_2O_4$ to give $Li_{1-x}[Mn^{3+}_{1+x}Mn^{4+}_{1-x}]O_4$, the concentration of Mn^{3+} becomes larger than the critical value for a tetragonal distortion. Thus it was demonstrated that a two-phase region existing for $0.1 \leq x \leq 0.8$ was responsible for a flat plateau at ~3 V in the open-circuit voltage versus composition of $Li_{1+x}Mn_2O_4$. The existence of this Jahn–Teller deformation of the spinel material, which is associated with an important anisotropic expansion of the unit cell, is a strong handicap with regard to a good cyclability in cathode materials (11). Recent strategies for developing highly reversible lithium-manganospinel cathode materials at 3 V have therefore aimed at overcoming the Jahn–Teller deformation by preparing Mn^{4+}-rich materials such as $Li_4Mn_5O_{12}$ and $Li_2Mn_4O_9$ (12).

In a quite recent article (28), Yamada and Tanaka observed, by means of differential scanning calorimetry (DSC) and X-ray diffraction, a reversible phase transition near 280 K for $Li[Mn_2]O_4$ that clearly reflects a first-order, cooperative Jahn–Teller distortion of the spinel from cubic to tetragonal symmetry. After cooling at $T < 267$ K and reheating to room temperature, the X-ray patterns showed a mixture of tetragonal (65%) and cubic (35%) phases. We undertook similar experiments (29) to investigate the sensitivity of the transition temperature T_t to the Mn^{3+} ion concentration on the B site of the $[Mn_{2-y}O_4]$ framework.

Figure 8 shows our DSC traces recorded on heating and cooling over the temperature interval 243–393 K for sample A3 ($n^+_{Mn} = 3.51$, $y = 2\delta = 0.002$) and sample A5 ($n^+_{Mn} = 3.61$, $y = 2\delta = 0.06$). Sample A3 clearly exhibits a reversible thermal effect around 20°C with a thermal hysterisis characteristic of a first-order phase change. On cooling, the transition occurs below room temperature, which explains why stoichiometric $Li[Mn_2]O_4$ samples cooled to room temperature have been reported to be cubic. On heating to room temperature from below 0°C, on the other hand, the sample is only partially converted

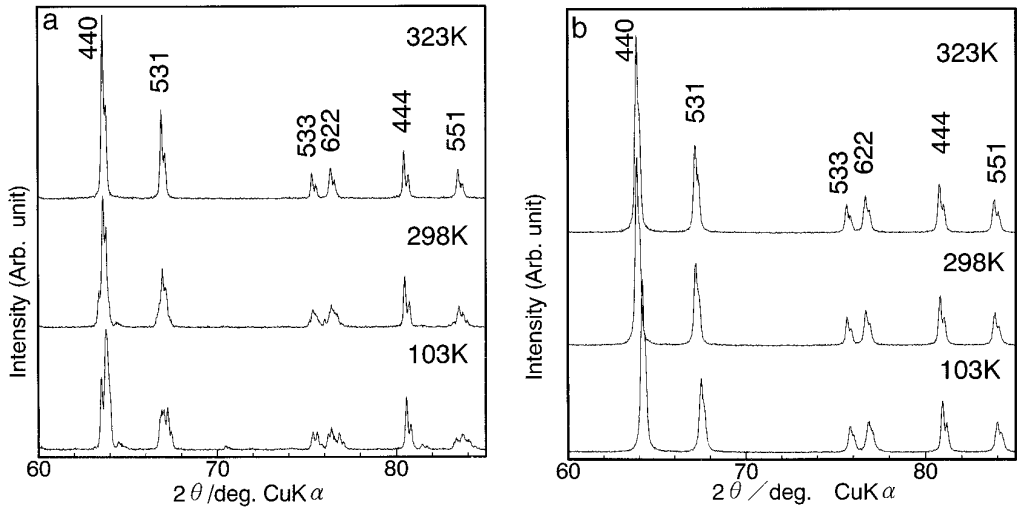

FIG. 9. Powder X-ray diffraction patterns of (a) stoichiometric $LiMn_2O_4$ and (b) $Li_{1.01}Mn_{1.94}O_4$ A5 first cooled down to 103 K and then heated up to 298 and 323 K. The cubic phase peak indexation is given in the *Fd3m* space group.

TABLE 3
Magnetic Characterization of Lithium Manganospinels

System	Sample	Synthesis temperature	n^{+}_{Mn}	a (Å)	μ_{eff} (μ_B per Mn atom)	Weiss constant θ (K)
$LiMn_2O_4$	A3	900	3.51	8.248	4.36	−266
	A7	900	3.56	8.239	4.33	−260
$Li_2Mn_4O_9$	A5	700	3.61	8.231	4.05	−220
	A4	400	3.69	8.204	3.94	−88
$LiMn_2O_4$	A3	900	3.51	8.248	4.36	−266
	B3	650	3.72	8.194	3.66	−61
$Li_4Mn_5O_{12}$	B4	650	3.84	8.167	3.47	+2
	B10	400	3.91	8.137	3.47	+40

back to the cubic phase. In contrast, no thermal effect is detected for the A5 sample $Li[Mn_{1.94}Li_{0.01}\square_{0.05}]O_4$ over all the temperature range studied. Sample A5 can also be written as $Li_{1.01}Mn^{3+}_{0.76}Mn^{4+}_{1.18}O_4$, and the reduction from 50% (as in $Li[Mn_2]O_4$) to 38% Mn^{3+} ions per (16*d*) site in the $[Mn_{2-y}O_4]$ spinel framework is sufficient to suppress the tetragonal distortion in the temperature interval 243–393 K. This demonstrates that T_t drops precipitously with the Mn^{3+} ion concentration per (16*d*) site as this concentration decreases from 0.5.

Figure 9 shows the X-ray diffraction patterns of the A3 (a) and A5 (b) samples recorded at different temperatures. The samples were first cooled down and the XRD patterns were recorded at 103, 298, and 323 K successively. The patterns of the A3 sample ($LiMn_2O_4$) clearly show that the cubic spinel peaks (except the (444) one) are split at 103K and also at 298 K, due to the appearance of the tetragonally distorted spinel phase below room temperature. The peak indexation indicates that sample A3, at 298 K, is actually a mixture of a cubic (a = 8.2458 (2) Å) and of a tetragonal (a = 5.8126 (6) Å, c = 8.2870 (12) Å) spinel phase. This observation fully confirms the DSC results presented above: when first cooled down below 0°C, $LiMn_2O_4$ still adopts a tetragonal structure at room temperature. Remarkably, the XRD pattern of the same A3 sample recorded at room temperature after cooling from 900°C does not show such a tetragonal distortion (Fig. 3). This is fully explained by taking into account the hysteresis phenomenon associated with the Jahn–Teller distortion. By contrast with the A3 sample, no peak splitting could be detected for the A5 sample, which remains cubic for the entire temperature range studied here. We demonstrated that a small alteration in the stoichiometry (particularly in the oxidation state of manganese) due to minor variations in the preparation process (starting materials, firing temperature) induced dramatic changes in the physicochemical properties of the lithium manganospinel materials.

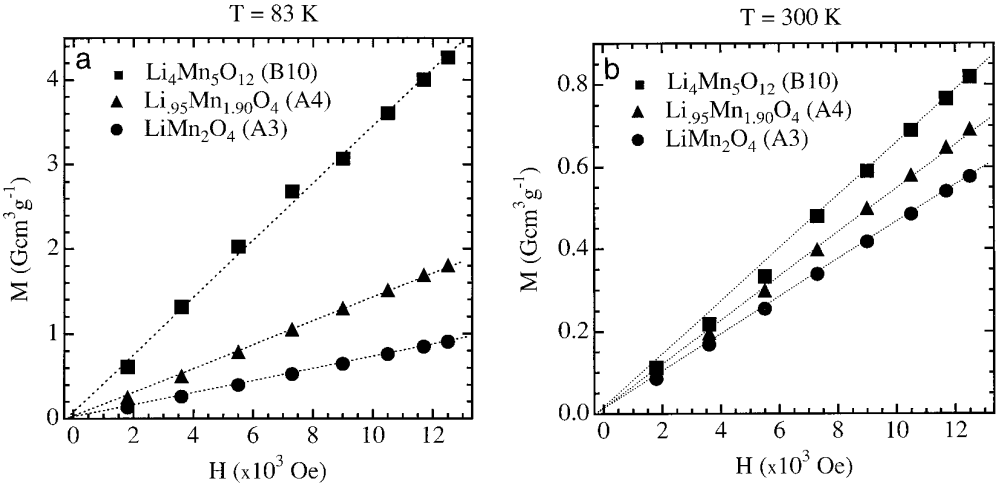

FIG. 10. Magnetization versus applied field H of lithium manganospinels at 83 K (a) and 300 K (b).

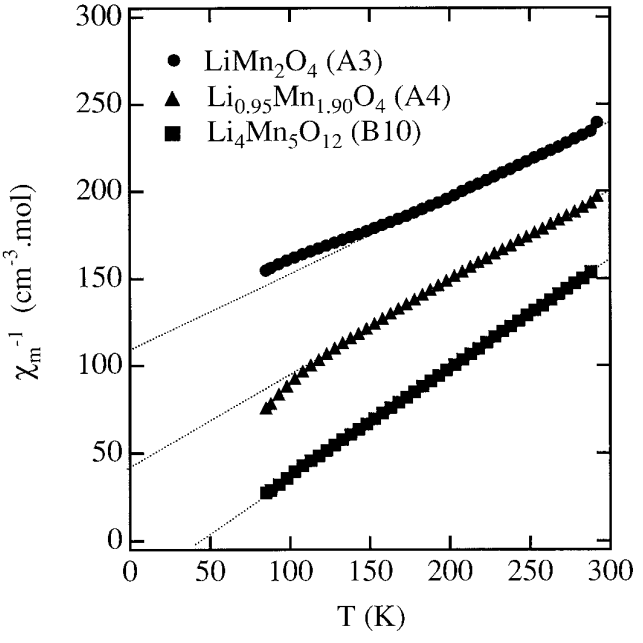

FIG. 11. Inverse molar magnetic susceptibility versus temperature for three characteristic lithium manganospinels, in the temperature range 83 K $\leq T \leq$ 300 K. Codes in brackets refer to sample labels described in Tables 1 and 2.

(*d*) *Magnetic Characterization of Lithium Manganospinels of the $LiMn_2O_4$–$Li_2Mn_4O_9$–$Li_4Mn_5O_{12}$ System*

Considerable work has been devoted, in the past, to the study of the magnetic properties of spinel materials. Blasse (30) has reported that $LiMn_2O_4$ (50% Mn^{3+}, 50% Mn^{4+}) remains paramagnetic down to 4.2 K with a large, negative Weiss constant ($\theta_A = -260$ K). The lack of a long-range magnetic order in the presence of strong antiferromagnetic Mn–Mn interactions can be understood as the result of frustration. Additionally, he showed that $Li_{0.5}Zn_{0.5}[Mn_{1.5}Li_{.5}]O_4$ (100% Mn^{4+}) is ferromagnetic ($\theta_A = +35$ K) due to 90° Mn^{4+}–O–Mn^{4+} positive interactions which, in this particular case, predominate against antiferromagnetic Mn–Mn interactions. On the other hand, Goodenough *et al.* reported that delithiation of $Li[Mn_2]O_4$ leaves an $[Mn_2]O_4$ spinel framework (with 100% Mn^{4+} also) that exhibits $\theta \sim -70$ K (31). It was of particular interest therefore to examine the magnetic behavior of lithium manganospinels of the $LiMn_2O_4$–$Li_2Mn_4O_9$–$Li_4Mn_5O_{12}$ system. This system, as discussed in detail in the previous paragraphs, provides several isostructural compositions with a continuous variation of the average oxidation state from $Mn^{3.5+}$ to Mn^{4+} on the octahedral (16*d*) crystallographic site.

Two series of compositions lying on the joins $LiMn_2O_4$–$Li_4Mn_5O_{12}$ and $LiMn_2O_4$–$Li_2Mn_4O_9$ were studied (Table 3). The field dependence of the magnetization measured at (a) 83 K and (b) 300 K for three representative samples, $LiMn_2O_4$ (A3), $Li_{.95}Mn_{1.9}O_4$ (defect spinel, A4) and $Li_4Mn_5O_{12}$ (stoichiometric spinel, B10), is shown in Fig. 10. All these three materials are paramagnetic above 83 K; no spontaneous magnetization is observed at zero field. The temperature dependence of the inverse molar magnetic susceptibility χ_m^{-1} of the three samples A3, A4, and B10 is depicted in Fig. 11. Above 100–150 K each plot may be represented by a straight line obeying the Curie–Weiss law $\chi_m^{-1} = (T - \theta)/C$. The values of the Weiss constant, obtained by extrapolation to $\chi_m^{-1} = 0$, vary from $\theta = -266$ K for $LiMn_2O_4$ to $\theta = +40$ K for $Li_4Mn_5O_{12}$. This agrees very satisfactorily with Blasse's earlier results on the signs of Mn–Mn interactions in lithium manganospinels (30). The experimental value of the effective magnetic moment (μ_{eff}) for nearly stoichiometric $LiMn_2O_4$ (sample A3) is very close to the theoretical one ($\mu_{eff} = 4.36\ \mu_B$) calculated in that case by assuming a mixed valence state consisting of 51% Mn^{4+} (μ_{eff} (spin only value) = 3.873 μ_B) and of 49% high-spin Mn^{3+} ($\mu_{eff} = 4.899\ \mu_B$). The values of the obtained magnetic moments for the lithium manganospinels decrease with increasing average oxidation state of manganese from 3.5+ to 4+, as depicted in Fig. 12. However, it is readily apparent that the experimental effective moments deviate noticeably from the theoretical ones (calculated by the simple model described above) especially for a higher average oxidation state of manganese. It would appear that in these compositions, which

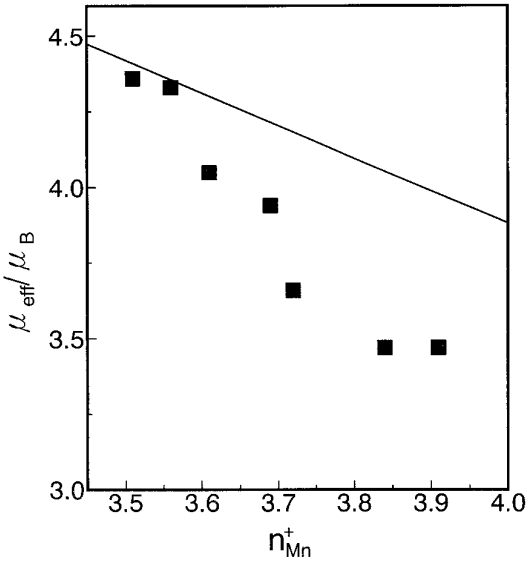

FIG. 12. Variation of the effective magnetic moment μ_{eff} with the average oxidation state of manganese for lithium manganospinels in the $LiMn_2O_4$–$Li_2Mn_4O_9$–$Li_4Mn_5O_{12}$ system. The solid line represents the theoretical values calculated on the basis of spin-only values of Mn^{3+} ($\mu_{eff} = 4.879\ \mu_B$) (high spin state) and Mn^{4+} ($\mu_{eff} = 3.873\ \mu_B$).

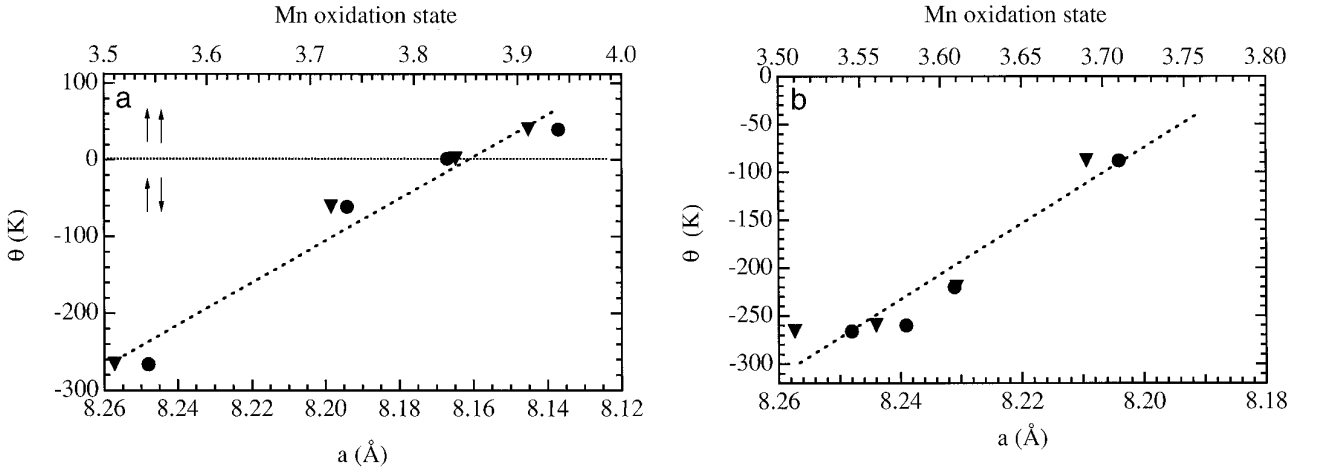

FIG. 13. Variation of the Weiss constant θ as a function of the average oxidation state of manganese (▼) or the cubic lattice parameter (●) for (a) stoichiometric spinel materials $Li_{1+\delta}Mn_{2-\delta}O_4$, $0 \le \delta \le 0.33$, and (b) nonstoichiometric spinel materials $Li_{1-\delta}Mn_{2-2\delta}O_4$, $0 \le \delta \le 0.047$. Parallel and antiparallel arrows refer to ferro- and antiferromagnetic behavior, respectively.

are near the crossover from $\theta < 0$ to $\theta > 0$, the Weiss constant is not temperature-independent, but decreases with increasing temperature:

$$\chi_m = C/[T - (\theta - \gamma T)] \qquad [9]$$

gives a $C_{eff} = C/(1 + \gamma)$ and a $\theta_{eff} = \theta/(1 + \gamma)$.

Figure 13 shows the variation of the Weiss constant with the cubic lattice parameter, i.e., with the average manganese oxidation state, for the two series of compositions lying on the joins $LiMn_2O_4$–$Li_4Mn_5O_{12}$ (Fig. 13a) and $LiMn_2O_4$–$Li_2Mn_4O_9$ (Fig. 13b). For both systems, we observe a rather regular increase of the Weiss constant with the manganese oxidation state, which reflects a progressive change in the relative strengths of the antiferromagnetic and the ferromagnetic interactions between Mn^{n+} cations in these lithium manganospinels. At this point, two components of the Mn–Mn interactions need to be distinguished:

(i) The antiferromagnetic Mn–Mn interaction between overlapping, half-filled t orbitals across a shared octahedral-site edge. Both Mn^{3+} (t^3e^1) and Mn^{4+} (t^3e^0), are half-filled t orbital cations. The strength of the Mn–Mn interactions increases sharply with decreasing lattice parameter, so it should be stronger for all Mn^{4+} ions, especially in λ-MnO_2 where the lattice parameter is particularly small.

(ii) The 90° Mn–O–Mn interactions take place via an O $2p$ orbital that σ bonds with an e obital on the Mn atom and π bonds with a t orbital on the neighboring Mn atom. The Mn^{4+} ions have empty e orbitals, so the 90° Mn^{4+}–O–Mn^{4+} interaction couples a half-filled t orbital with an empty e orbital, which gives a ferromagnetic interaction according to the Goodenough–Kanamori superexchange rules. The Mn^{3+} ions, on the other hand, have partially filled e orbitals, and the Pauli exclusion principle requires antiferromagnetic 90° Mn–O–Mn coupling for interactions between Mn^{3+} ions and between a Mn^{3+} and a Mn^{4+} ion in the absence of a static Jahn–Teller deformation.

From the above considerations, the progressive passage from antiferromagnetic to ferromagnetic behavior when the average oxidation state of Mn is increased from 3.5+ to 4+ can be explained as follows. $LiMn_2O_4$ shows a strongly negative θ value ($\theta = -266$ K) due to the addition of (i) antiferromagnetic Mn^{3+}–Mn^{4+} and (ii) antiferromagnetic

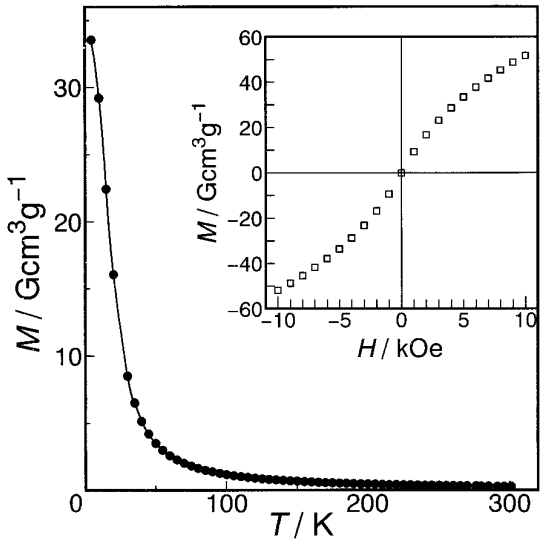

FIG. 14. Temperature dependence of the magnetization for $Li_4Mn_5O_{12}$ (B10). The field dependence of the magnetization at 5 K is also shown.

90° Mn^{3+}–O–Mn^{4+} interactions. Substitution of Mn^{4+} for Mn^{3+} generates ferromagnetic 90° Mn^{4+}–O–Mn^{4+} interactions which, in the case of $Li_4Mn_5O_{12}$ where the lattice parameter a is not too small, dominate against the antiferromagnetic Mn^{4+}–Mn^{4+} interactions. This has to be compared, interestingly, with the magnetic behavior reported for the λ-$[Mn_2]O_4$ spinel framework for which the antiferromagnetic Mn^{4+}–Mn^{4+} interaction dominates due to a much smaller lattice parameter $a = 8.08$ Å (31). The positive value of θ for $Li_4Mn_5O_{12}$ ($\theta = +40$ K) is indicative of ferromagnetic behavior below 83 K, as demonstrated by the variation of the magnetization with the temperature between 5 and 300 K (Fig. 14). An important increase of the magnetization is observed below 50 K and the occurrence of a spontaneous magnetization at 5 K reflects the ferromagnetic order. This magnetic behavior for $Li_4Mn_5O_{12}$, which can alternately be written as $Li_{1.0}[Mn_{1.67}Li_{0.33}]O_4$, is very similar to the one reported for $Li_{0.5}Zn_{0.5}[Mn_{1.5}Li_{0.5}]O_4$ (30), where the oxidation state of manganese is also equal to 4+. In the $LiMn_2O_4$–$Li_2Mn_4O_9$ system (Fig. 13b), we observe also a rather regular increase of the Weiss constant θ with the manganese oxidation state, up to $\theta = -82$ K for $Li_{0.95}Mn_{1.9}O_4$ ($n^+_{Mn} = 3.69$). From the considerations described above, we can also reasonably expect, for the end-member $Li_2Mn_4O_9$, $n^+_{Mn} = 4$, a ferromagnetic behavior.

CONCLUSION

The stoichiometry of the lithium manganospinels of interest as cathode materials for rechargeable lithium batteries is highly dependent on the preparation route (Mn sources, Li salts, and reaction temperature) adopted. We demonstrated that X-ray diffraction and chemical analysis of the Li/Mn ratio and Mn oxidation state provide powerful tools for controlling the exact composition of these spinels. The precise control and knowledge of these lithium manganospinels is in fact of particular importance for a complete understanding of their electrochemical properties in a lithium battery system. Stoichiometric $LiMn_2O_4$ shows a reversible phase transition at 30°C upon heating and 10°C upon cooling, that is associated with a tetragonal–cubic distortion. Creation of lithium and manganese vacancies ($LiMn_2O_4$–$Li_2Mn_4O_9$ join) or substitution of lithium for manganese on the 16*d* octahedral sites ($LiMn_2O_4$–$Li_4Mn_5O_{12}$ join) leads to higher values of the average oxidation state of manganese, between 3.5+ and 4+. Reduction of the Mn^{3+}–ion concentration results in (i) the suppression of the Jahn–Teller distortion and (ii) a progressive passage from antiferromagnetic ($LiMn_2O_4$, $\theta = -266$ K, $n^+_{Mn} = 3.5$) to ferromagnetic behavior ($Li_4Mn_5O_{12}$, $\theta = +40$ K, $n^+_{Mn} = 4.0$), where the lattice parameter is not too small.

ACKNOWLEDGMENT

The authors gratefully acknowledge financial support from the Science and Technology Agency, Japan, and the Robert A. Welch Foundation, Houston, Texas. The authors also thank A. Manthiram and J. Töpfer for helpful suggestions concerning the manganese redox titration.

REFERENCES

1. T. Mizushima, P. C. Jones, P. J. Wiseman, and J. B. Goodenough, *Mater. Res. Bull.* **15,** 783 (1980).
2. T. Nagaura, "4th International Rechargeable Battery Seminar, Dearfield Beach, Florida, 1991." Vol. 10, p. 209.
3. J. B. Goodenough, M. M. Thackeray, W. I. F. David, and P. G. Bruce, *Rev. Chim. Miner.* **21,** 435 (1984).
4. M. M. Thackeray, W. I. F. David, and J. B. Goodenough, *Mater. Res. Bull.* **17,** 785 (1982).
5. M. M. Thackeray, W. I. F. David, P. G. Bruce, and J. B. Goodenough, *Mater. Res Bull.* **18,** 461 (1983).
6. M. M. Thackeray, P. J. Johnson, L. A. de Piciotto, P. G. Bruce, and J. B. Goodenough, *Mater. Res Bull.* **19,** 179 (1984).
7. D. Guyomard and J. M. Tarascon, *J. Electrochem. Soc.* **139,** 937 (1992).
8. J. M. Tarascon and D. Guyomard, *Electrochim. Acta* **38,** 1221 (1993).
9. D. Guyomard and J. M. Tarascon, *Solid State Ionics* **69,** 222 (1994).
10. M. N. Richard, E. W. Fuller, and J. R. Dahn, *Solid State Ionics* **73,** 81 (1994).
11. M. M. Thackeray, *J. Electrochem. Soc.* **142,** 2568 (1995).
12. M. M. Thackeray, A. de Kock, M. H. Rossouw, D. Liles, R. Bittihu, and D. Hoge, *J. Electrochem. Soc.* **139,** 363 (1992).
13. R. J. Gummow, A. De Kock, and M. M. Thackeray, *Solid State Ionics* **69,** 59–67 (1994).
14. A. de Kock, M. H. Rossouw, L. A. de Picciotto, M. M. Thackeray, W. I. F. David, and R. M. Ibberson, *Mater. Res. Bull.* **25,** 657 (1990).
15. W. J. Macklin, R. J. Neat, and R. J. Powell, *J. Power Sources* **34,** 39 (1991).
16. M. M. Thackeray, M. H. Rossouw, A. de Kock, A. P. de la Harpe, R. J. Gummow, K. Pearce, and D. C. Liles, *J. Power Sources* **43–44,** 289 (1993).
17. T. Ohzuku, A. Ueda, and T. Hirai, *Chem. Express* **7,** 193, (1992).
18. R. J. Gummow and M. M. Thackeray, *J. Electrochem. Soc.* **141,** 1178 (1992).
19. J. N. Reimers, E. W. Fuller, E. Rossen, and J. R. Dahn, *J. Electrochem. Soc.* **140,** 3396 (1993).
20. R. J. Gummow, D. C. Liles, and M. M. Thackeray, *Mater. Res. Bull.* **28,** 1249 (1993).
21. I. Koetschau, M. N. Richard, J. R. Dahn, J. B. Soupart, and J. C. Rousche, *J. Electrochem. Soc.* 142, 2906 (1995).
22. Y. Xia, H. Noguchi, and M. Yoshio, *J. Solid State Chem.* **119,** 216 (1995).
23. D. G. Wickham and E. R. Whipple, *Talanta* **10,** 314 (1963).
24. A. Masbah, A. Verbaux, and M. Tournoux, *Mater. Res. Bull.* **18,** 1375 (1983).
25. T. Takada, H. Hakayama, and E. Akiba, *J. Solid State Chem.* **115,** 420 (1995).
26. K. S. Nanjundaswamy, personal communication.
27. J. B. Goodenough and A. L. Loeb, *Phys. Rev.* **98**(2), 391 (1955).
28. A. Yamada, and M. Tanaka, *Mater. Res. Bull.* **30**(6), 715 (1995).
29. M. Tabuchi *et al.*, in preparation.
30. G. Blasse, *J. Phys. Chem. Solids* **27,** 383 (1966).
31. J. B. Goodenough, A. Manthiram, A. C. W. P. Jones, and P. Strobel, *MRS Symp. Proc.* **135,** 391 (1989).
32. J. B. Goodenough, "Magnetism and the Chemical Bond." Wiley, New York/London, 1963.